

Cosmological Constraint on Vector Mediator of Neutrino-Electron Interaction in light of XENON1T Excess

Masahiro Ibe^{a,b}, Shin Kobayashi^a, Yuhei Nakayama^a and Satoshi Shirai^b

^a *ICRR, The University of Tokyo, Kashiwa, Chiba 277-8582, Japan*

^b *Kavli Institute for the Physics and Mathematics of the Universe (WPI),
The University of Tokyo Institutes for Advanced Study,
The University of Tokyo, Kashiwa 277-8583, Japan*

Abstract

Recently, the XENON1T collaboration reported an excess in the electron recoil energy spectrum. One of the simplest new physics interpretation is a new neutrino-electron interaction mediated by a light vector particle. However, for the parameter region favored by this excess, the constraints from the stellar cooling are severe. Still, there are astrophysical uncertainties on those constraints. In this paper, we discuss the constraint on the light mediator from the effective number of neutrino N_{eff} in the CMB era, which provides an independent constraint. We show that N_{eff} is significantly enhanced and exceeds the current constraint in the parameter region favored for the XENON1T excess. As a result, the interpretation by a light mediator heavier than about 1 eV is excluded by the N_{eff} constraint.

1 Introduction

The XENON1T experiment has recently reported an excess in the electron recoil energy spectrum above the known expected background spectrum [1]. Although the XENON1T experiment has not excluded unknown backgrounds, such as the β -decay of the tritium, the report is intriguing and has prompted many new physics interpretations.

Among various new physics, one of the simplest possibilities is to introduce non-standard neutrino-electron interactions so that the solar neutrino flux explains the excess [2–8]. For example, the XENON1T has discussed the sizable neutrino magnetic moment as a candidate for such a non-standard interaction. However, the best fit value is in tension with constraints from the white dwarfs and the globular clusters [9]. Refs. [3–8] have discussed new neutrino-electron interactions mediated by a light mediator, where the mediator with a mass below $\mathcal{O}(100)$ keV and the neutrino-electron coupling, $(g_e g_\nu)^{1/2} \sim 3 \times 10^{-7}$ explains the excess. The effects on the stellar cooling severely constrain the coupling constant of the light mediator [10–15]. However, those astrophysical constraints are still under debate as there are several uncertainties in the case of the mediator heavier than 1 eV [12, 16]. For example, a new mediator produced inside the astronomical objects is re-absorbed before exiting the objects in the case of a large coupling to electron, which weakens the constraints.

In this paper, we discuss a new constraint on the light mediator from the effective number of neutrino degrees of freedom, N_{eff} , measured by the cosmic microwave background (CMB) observations. In the standard cosmology, it is predicted that $N_{\text{eff}}^{(\text{SM})} \simeq 3.045$ [17, 18], which is consistent with the current CMB measurement. The introduction of new physics alters the N_{eff} prediction, which provides a constraint independent from the astrophysical constraints. As the light mediator interpretation of the XENON1T excess requires a particle lighter than $\mathcal{O}(100)$ keV, the mediator mainly decays into the neutrinos. As we will see, the presence of the mediator significantly enhances N_{eff} even for a very tiny coupling $g \sim 10^{-10}$. The parameter region favored for the XENON1T excess results in $N_{\text{eff}} > 5$ for $m_{Z'} \geq 1$ eV, which exceeds the upper limit of the Planck CMB only (joint Planck+BAO) constraint, $N_{\text{eff}} = 2.92^{+0.36}_{-0.37}$ ($2.99^{+0.34}_{-0.33}$) at 95% C.L. [19].

The organization of the paper is as follows. In Sec. 2, we explain the setup of the phenomenological model for the light mediator interpretation of the XENON1T excess. In Sec. 3, we show the full Boltzmann equation of the momentum distribution of the light mediator. In Sec. 4, we obtain the constraints on the neutrino and the electron coupling of the light mediator. The final section is devoted to our conclusions.

2 Setup

As a phenomenological setup, we consider a light vector boson which couples to the neutrinos ν_i and the charged leptons ψ_i ,

$$\mathcal{L}_{Z'} = g_\nu^{ij} Z'_\mu \nu_{L,i}^\dagger \bar{\sigma}^\mu \nu_{L,j} + g_\ell Z'_\mu \bar{\psi}_\ell \gamma^\mu \psi_\ell, \quad (1)$$

where $i, j, \ell = e, \mu, \tau$, $\nu_{L,i}$ is a left-handed 2-component Weyl spinor and ψ_ℓ is a 4-component Dirac spinor.¹ The new vector mediator Z' has a mass $m_{Z'}$. Hereafter, we assume that the mediator is lighter than an electron-positron pair, $m_{Z'} < 2m_e$, which is favored by the XENON1T excess [3]. Accordingly, the decay into the e^\pm is kinematically forbidden.

As the left-handed charged leptons and the neutrinos are in the same multiplets in the Standard Model (SM), simple introduction of a new $U(1)$ gauge interaction tends to predict $g_\nu = g_\ell$. It is, however, possible to achieve $g_\nu \gg g_\ell$ in, for example, the $U(1)_{L_\mu-L_\tau}$ gauge symmetry [20, 21]. In this case, g_ν corresponds to the $U(1)_{L_\mu-L_\tau}$ gauge coupling, while g_e is provided through the gauge kinetic mixing between the $U(1)_{L_\mu-L_\tau}$ gauge boson and the photon which leads to $g_\nu \simeq 70g_e$ [22]. The dark photon coupling to the SM gauge bosons through the kinetic mixing also predicts hierarchical coupling constants, $g_\nu \sim m_{Z'}^2/m_Z^2 \times g_e$ [23]. More generally, the dark photon with non-trivial $U(1)_X$ gauge charge assignment to the SM fermions lead to gauge couplings, $g_e \sim g_X - \epsilon e$ and $g_\nu \sim g_X$, which can be tuned either $g_\nu \gg g_e$ or $g_e \gg g_\nu$. Here, e and g_X are the QED and $U(1)_X$ gauge coupling constants, and ϵ is the kinetic mixing parameter between field strengths, i.e., $\epsilon F_{\text{QED}}^{\mu\nu} F_{X\mu\nu}$.² In the following, we take g_ν and g_e to be independent free parameters. We also assume that the mediator couples to one flavor of the neutrinos. Since the neutrino oscillation is fast enough for $T < \mathcal{O}(1)$ MeV, the choice of the neutrino flavor is irrelevant for the following arguments.

Now, let us discuss cosmology of the mediator at the temperature below $\mathcal{O}(10)$ MeV, which is crucial for the determination of N_{eff} . In this setup, the mediators are produced from the thermal bath through, $e^- + e^+ \leftrightarrow \gamma + Z'$, $e^\pm + \gamma \leftrightarrow e^\pm + Z'$, $\nu + \nu \leftrightarrow Z'$, and $\nu + \nu \leftrightarrow Z' + Z'$ (see Fig. 1). These production processes are relatively enhanced compared to the Hubble expansion rate as the temperature decreases. Hence, the mediator is produced at the lower temperature even if it has the zero initial abundance after inflation. In our analysis, we adopt this “freeze-in” scenario, which leads to the most conservative constraint.

In order to comprehend the overview of the cosmology, let us estimate the temperature at which the production processes become effective. For the electron annihilation or scattering production, if

$$\Gamma_{e^-e^+ \rightarrow \gamma Z'}(T) \sim e^2 g_e^2 T \gtrsim H(T), \quad (2)$$

¹Depending on the ultraviolet completion of the massive gauge boson, there can be higher dimensional operators. In the following analysis, we neglect such interactions.

²The hierarchical coupling condition ($g_e \gg g_\nu$ or $g_\nu \gg g_e$) is stable against the radiative corrections. The stability of $g_e \gg g_\nu$ is trivial once we impose $g_\nu = 0$ as the on-shell renormalization condition, because the neutrinos do not couple to the photon nor Z' at any order. The stability of $g_\nu \gg g_e$ is clarified by the conjugation symmetry of QED. The charge conjugation symmetry forbids the mixing term once we impose $g_e = 0$. Thus, the radiatively generated mixing term is proportional to g_e , and hence, the hierarchical coupling is technically natural.

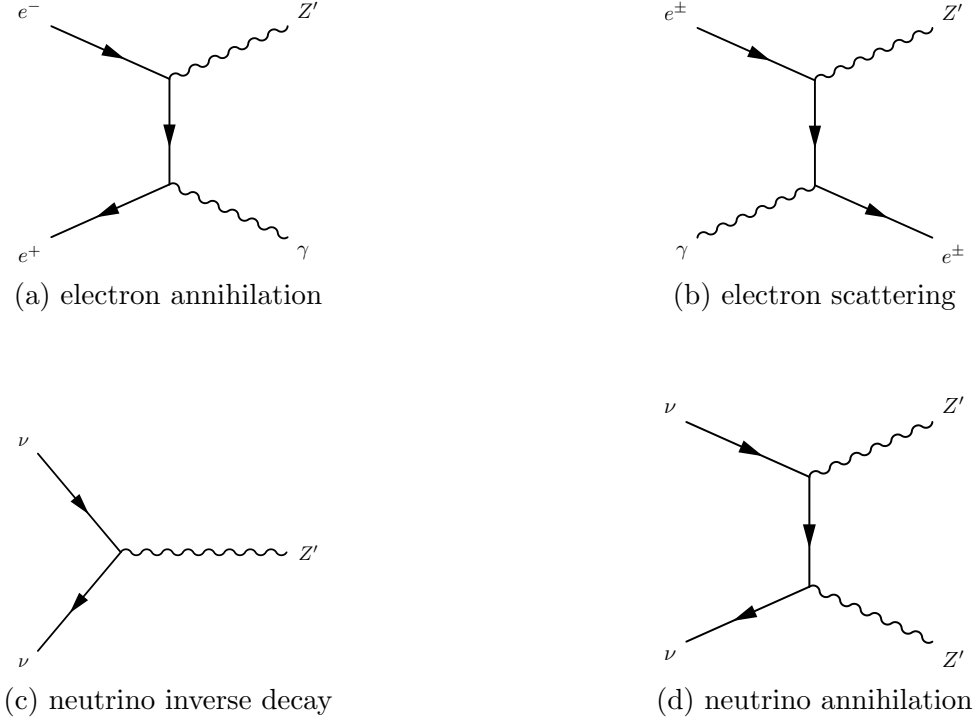


Figure 1: The Feynman diagrams relevant for the Z' production.

that is,

$$T \lesssim e^2 g_e^2 M_{\text{Pl}} , \quad (3)$$

these processes are effective. Here, H is the Hubble expansion rate and M_{Pl} is the reduced Planck scale. Thus, the dark photon is thermalized with the γ - e thermal bath before the e^\pm annihilation for

$$g_e \gg 10^{-9} . \quad (4)$$

In this region, Z' and e^\pm are thermalized together and share the same temperature.

For the production via the neutrino annihilation, it becomes efficient for

$$\Gamma_{\nu\nu \rightarrow Z'Z'}(T) \sim g_\nu^4 T \gtrsim H(T) \quad \therefore T \lesssim g_\nu^4 M_{\text{Pl}} . \quad (5)$$

Thus, Z' and ν are thermalized by the temperature, $T \sim m_{Z'}$, for

$$g_\nu \gg 10^{-6} \left(\frac{m_{Z'}}{1 \text{ keV}} \right)^{1/4} . \quad (6)$$

As we consider $m_{Z'} < 2m_e$, the mediator mainly decays into a pair of neutrinos. The decay rate at the temperature $T \gtrsim m_{Z'}$ is given by

$$\Gamma_{Z' \rightarrow \nu\nu}(T) \sim \Gamma_{Z' \rightarrow \nu\nu}^0 \times \frac{m_{Z'}}{T} . \quad (7)$$

Here, $\Gamma_{Z' \rightarrow \nu\nu}^0$ denotes the partial decay rate of Z' into one flavor of the three neutrinos at the Z' rest frame,

$$\Gamma_{Z' \rightarrow \nu\nu}^0 = \frac{1}{24\pi} g_\nu^2 m_{Z'} . \quad (8)$$

In the following, we assume that the mediator couples to one flavor of the three neutrinos. We also treat the neutrinos massless throughout this paper. The light mediator exhibits the in-equilibrium decay at the neutrino temperature T_ν is of $\mathcal{O}(m_{Z'})$ for

$$g_\nu \gg 5 \times 10^{-12} \left(\frac{m_{Z'}}{1 \text{ keV}} \right)^{1/2} . \quad (9)$$

Note that if g_ν is between Eqs. (6) and (9), only the inverse decay is effective. In this case, the neutrino thermal bath may have a non-zero chemical potential due to the number conservation of Z' and ν [24, 25].

When Z' thermalization occurs by the neutrino decoupling era, the energy injected into the ν sector changes the ratio of the neutrino and the photon energy densities, ρ_ν/ρ_γ , from the one in the standard cosmology. In this case, N_{eff} is changed drastically, which conflicts with the CMB observations.

For the summary of this section, we show the temperature dependence of the production rates of Z' in Fig. 2. Here we define the production rates per unit volume, $\Gamma_{Z'\text{-prod}}$, as

$$\Gamma_{Z'\text{-prod}} = \int \frac{d^3 p_{Z'}}{(2\pi)^3} f_{Z'}^{\text{BE}} \tilde{G}_{Z'} , \quad (10)$$

where $\tilde{G}_{Z'}$ is a collision term defined in Eqs. (13), (14), (15), (18), and (19) in the next section. We also normalize the production rate with Hs , where H is the Hubble expansion rate and s is the entropy density of the Universe. If the production rate exceeds the expansion rate, i.e., $\Gamma_{Z'\text{-prod}}/(Hs) \gtrsim 1$, Z' production from the SM thermal bath becomes efficient.

3 Boltzmann equations

We solve the Boltzmann equation of the phase space distribution of Z' , $f_{Z'}$, the energy densities of the γ - e thermal bath, $\rho_{\gamma e}$, the neutrino thermal bath, ρ_ν and the number density of the neutrino thermal bath, n_ν . Here, we need to treat ρ_ν and n_ν independently, since the neutrino thermal bath obtains a non-vanishing chemical potential from the Z' interaction as we will see later. Hereafter, we assume that γ has the Bose-Einstein distribution, and e^\pm and ν have the Fermi-Dirac distributions, which gives a good approximation after the neutrino decoupling [24–26]. We treat the three flavor neutrinos as a fluid with a single temperature/chemical potential to mimic the effect of the neutrino oscillations as in Refs. [24–26].

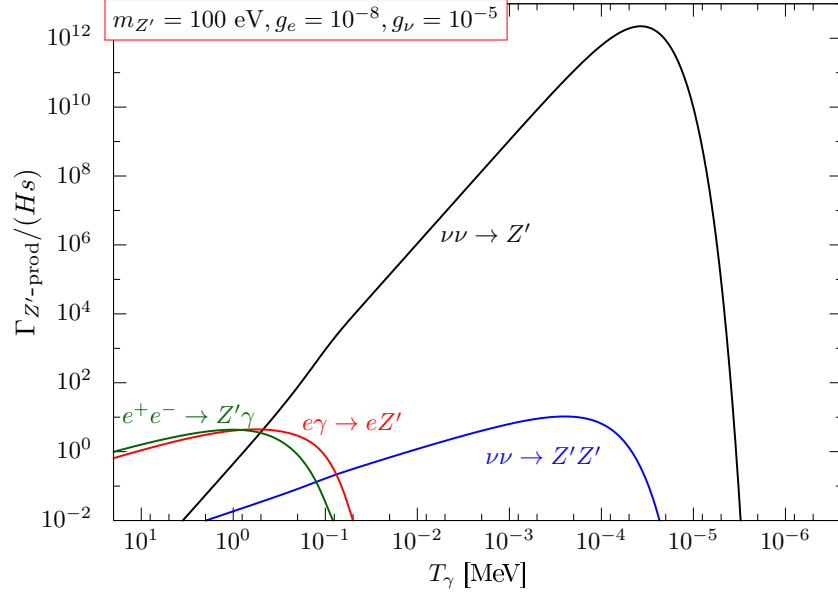


Figure 2: The temperature dependence of the production rates of the modes $e\gamma \rightarrow eZ'$ (red), $e^+e^- \rightarrow Z'\gamma$ (green), $\nu\nu \rightarrow Z'$ (black) and $\nu\nu \rightarrow Z'Z'$ (blue).

The evolution of the momentum distribution for the mediator Z' is determined by the Boltzmann equation,

$$\frac{\partial f_{Z'}}{\partial t} - Hp \frac{\partial f_{Z'}}{\partial p} = -\mathcal{C}[f_{Z'}] , \quad (11)$$

where H is the Hubble expansion rate and $\mathcal{C}[f_{Z'}]$ is a sum of collision terms. In this work, we include the decay, the scattering and the annihilation processes for the calculation of the collision terms. With the aid of the formalism in Ref. [23], all the Z' collision terms are written in the approximated form

$$\begin{aligned} \mathcal{C}[f_{Z'}] \simeq & \tilde{G}_{Z' \leftrightarrow \nu\nu} (f_{Z'} - f_{Z'}^{\text{BE}}(T_\nu, 2\mu_\nu)) + (\tilde{G}_{Z'Z' \leftrightarrow \nu\nu} f_{Z'} - \tilde{G}_{Z'Z' \leftrightarrow \nu\nu}^{\text{eq}}) \\ & + \tilde{G}_{e^\pm Z' \leftrightarrow e^\pm \gamma} (f_{Z'} - f_{Z'}^{\text{BE}}(T_\gamma, 0)) + \tilde{G}_{\gamma Z' \leftrightarrow e^- e^+} (f_{Z'} - f_{Z'}^{\text{BE}}(T_\gamma, 0)) \\ & + \tilde{G}_{Z' \leftrightarrow 3\gamma} (f_{Z'}(E_{Z'}) - f_{Z'}^{\text{BE}}(T_\gamma, 0)) . \end{aligned} \quad (12)$$

Here, $f_{Z'}^{\text{BE}}$ is the Bose-Einstein distribution function for a single degree of freedom of Z' , μ_ν is a chemical potential of the neutrino, and T_γ, T_ν are the temperatures of the γ - e and the neutrino

thermal bathes, respectively. Each term for the process including neutrinos is written as

$$\tilde{G}_{Z' \leftrightarrow \nu\nu} = \frac{m_{Z'} \Gamma_{Z' \rightarrow \nu\nu} (1 + \varphi(T_\nu, \mu_\nu, p_{Z'}))}{E_{Z'}} , \quad (13)$$

$$\begin{aligned} \tilde{G}_{Z' Z' \leftrightarrow \nu\nu} &= \frac{1}{512\pi^3} \frac{1}{|\mathbf{p}_{Z'}| E_{Z'}} \int d\tilde{E}_{Z'} [f_{Z'}(\tilde{E}_{Z'}) - (1 + f_{Z'}(\tilde{E}_{Z'})) e^{-(E_{Z'} + \tilde{E}_{Z'})/T_\nu} e^{2\mu_\nu/T_\nu}] \\ &\quad \times \int ds \frac{1}{\sqrt{s} |\mathbf{p}_{Z'Z'}^{\text{cms}}|} \int dt |\bar{\mathcal{M}}_{Z' Z' \leftrightarrow \nu\nu}|^2 \times 12 , \end{aligned} \quad (14)$$

$$\begin{aligned} \tilde{G}_{Z' Z' \leftrightarrow \nu\nu}^{\text{eq}} &= \frac{1}{512\pi^3} \frac{1}{|\mathbf{p}_{Z'}| E_{Z'}} \int d\tilde{E}_{Z'} [(1 + f_{Z'}(\tilde{E}_{Z'})) e^{-(E_{Z'} + \tilde{E}_{Z'})/T_\nu} e^{2\mu_\nu/T_\nu}] \\ &\quad \times \int ds \frac{1}{\sqrt{s} |\mathbf{p}_{Z'Z'}^{\text{cms}}|} \int dt |\bar{\mathcal{M}}_{Z' Z' \leftrightarrow \nu\nu}|^2 \times 12 . \end{aligned} \quad (15)$$

Here, we define

$$\varphi(T_\nu, \mu_\nu, p_{Z'}) = \frac{m_{Z'} T_\nu}{p_{Z'} p_\nu^0} \log \left(\frac{e^{(E_{Z'} E_\nu^0 - \mu_\nu m_{Z'})/(T_\nu m_{Z'})} + e^{-p_{Z'} p_\nu^0/(T_\nu m_{Z'})}}{e^{(E_{Z'} E_\nu^0 - \mu_\nu m_{Z'})/(T_\nu m_{Z'})} + e^{p_{Z'} p_\nu^0/(T_\nu m_{Z'})}} \right) , \quad (16)$$

where $p_\nu^0 = E_\nu^0 = m_{Z'}/2$ are the momentum and energy of the neutrino at the rest frame of the dark photon, Z' . For collision terms of the $\nu\nu$ annihilation processes, we use the integrated amplitude

$$\begin{aligned} \int ds \frac{1}{\sqrt{s} |\mathbf{p}_{Z'Z'}^{\text{cms}}|} \int dt |\bar{\mathcal{M}}_{Z' Z' \leftrightarrow \nu\nu}|^2 &= -\frac{8}{9} g_\nu^4 m_{Z'}^2 [(x_+ - x_-) + 2(f(y_+) - f(y_-))] , \\ f(y) &= \frac{1}{2y^2} + \frac{y^2}{2} + \frac{\log(y)}{y^2} - y^2 \log(y) - 4 \log(y)^2 + 4 \int_{y^2}^\infty dz \frac{\log(z)}{z^2 + 1} , \\ x_\pm &= \left(\frac{E_{Z'}}{m_{Z'}} + \frac{\tilde{E}_{Z'}}{m_{Z'}} \right)^2 \pm \sqrt{\left(\frac{E_{Z'}}{m_{Z'}} \right)^2 - 1} \sqrt{\left(\frac{\tilde{E}_{Z'}}{m_{Z'}} \right)^2 - 1} , \\ y_\pm &= \frac{1}{2} (\sqrt{x_\pm} + \sqrt{x_\pm - 4}) . \end{aligned} \quad (17)$$

For the scattering process with the γ - e thermal bath, we use the same formulae in the appendix of Ref. [23] with parameters replaced as $\varepsilon g \rightarrow g_e, m_{\gamma'} \rightarrow m_{Z'}$,

$$\tilde{G}_{e^\pm Z' \leftrightarrow e^\pm \gamma} = \frac{1}{512\pi^3} \frac{T e^{-E_{Z'}/T}}{|\mathbf{p}_{Z'}| E_{Z'} f_{Z'}^{\text{BE}}(E_{Z'})} \int ds \frac{1}{\sqrt{s} |\mathbf{p}_{eZ'}^{\text{cms}}|} \log \left[\frac{1 + e^{-E_e^-/T}}{1 + e^{-E_e^+/T}} \right] \int dt |\bar{\mathcal{M}}_{e^\pm \gamma \leftrightarrow e^\pm Z'}|^2 \times 8 , \quad (18)$$

$$\tilde{G}_{\gamma Z' \leftrightarrow e^- e^+} = \frac{1}{512\pi^3} \frac{T e^{-E_{Z'}/T}}{|\mathbf{p}_{Z'}| E_{Z'} f_{Z'}^{\text{BE}}(E_{Z'})} \int ds \frac{1}{\sqrt{s} |\mathbf{p}_{\gamma Z'}^{\text{cms}}|} \log \left[\frac{1 - e^{-E_\gamma^+/T}}{1 - e^{-E_\gamma^-/T}} \right] \int dt |\bar{\mathcal{M}}_{e^+ e^- \leftrightarrow \gamma Z'}|^2 \times 8 , \quad (19)$$

$$\tilde{G}_{Z' \leftrightarrow 3\gamma} = \frac{m_{Z'}}{E_{Z'}} \Gamma_{Z' \rightarrow 3\gamma} = \frac{17 g_e^2 \alpha^3}{2^9 3^6 5^3 \pi^4} \frac{m_{Z'}^9}{m_e^8} \mathcal{F}(m_{Z'}^2/m_e^2) . \quad (20)$$

In the above, we define $|\bar{\mathcal{M}}|^2$ as the amplitude squared averaged over spins of all the initial and final states. Thus, we multiply factors of spin degrees of freedom when we integrate $|\bar{\mathcal{M}}|^2$ over phase space volumes. The factor $\mathcal{F}(x)$ in the $3\text{-}\gamma$ decay process is given in Ref. [27].

We determine the thermal evolution of the SM particles by solving the zeroth and first moment of the Boltzmann equations,

$$\frac{dn_\nu}{dt} = -3Hn_\nu - C_{e\leftrightarrow\nu}^{(0)}(T_\gamma, T_\nu, \mu_\nu) + 2C_{Z'\rightarrow\nu_e\bar{\nu}_e}^{(0)}(T_\nu, \mu_\nu) + C_{Z'Z'\rightarrow\nu_e\bar{\nu}_e}^{(0)}(T_\nu, \mu_\nu) , \quad (21)$$

$$\frac{d\rho_\nu}{dt} = -4H\rho_\nu - C_{e\leftrightarrow\nu}^{(1)}(T_\gamma, T_\nu, \mu_\nu) + C_{Z'\rightarrow\nu_e\bar{\nu}_e}^{(1)}(T_\nu, \mu_\nu) + C_{Z'Z'\rightarrow\nu_e\bar{\nu}_e}^{(1)}(T_\nu, \mu_\nu) , \quad (22)$$

$$\frac{d\rho_{\gamma e}}{dt} = -3H(\rho_{\gamma e} + p_{\gamma e}) + C_{e\leftrightarrow\nu}^{(1)}(T_\gamma, T_\nu, \mu_\nu) + C_{eZ'\leftrightarrow e\gamma}^{(1)}(T_\gamma) + C_{\gamma Z'\leftrightarrow e^-e^+}^{(1)}(T_\gamma) + C_{Z'\leftrightarrow 3\gamma}^{(1)}(T_\gamma) , \quad (23)$$

where $C^{(n)}$ is the n -th energy moment of a collision term. Here, $n_\nu = n_{\nu_e} + n_{\nu_\mu} + n_{\nu_\tau}$ and $\rho_\nu = \rho_{\nu_e} + \rho_{\nu_\mu} + \rho_{\nu_\tau}$ are the number and energy density of the neutrinos, and $\rho_{\gamma e}$ and $p_{\gamma e}$ are the density and pressure of the γ - e thermal bath, which include thermal corrections [28–30]. For the processes including Z' , we integrate the each term of the right hand side of Eq.(12) to obtain $C^{(n)}$. Following the procedure of Ref. [25], we have included the effect of spin-statistics and the electron mass in the collision terms between e^\pm and the neutrinos, $C_{e\leftrightarrow\nu}^{(0)}$ and $C_{e\leftrightarrow\nu}^{(1)}$, which are summarized in the Appendix A.

The neutrino momentum distributions depart from the Fermi-Dirac distributions at low temperatures unless the reaction $Z \leftrightarrow \nu$ is thermalized [17, 24]. The above approximation is validated in Ref. [25] by comparing with the full solution of the Boltzmann equation of the neutrino distributions, which shows the accuracy is better than 0.04%.

The new interactions in $\mathcal{L}_{Z'}$ also induces a new channel of ν - e scattering via the off-shell Z' exchange. As shown in Ref. [3], however, rather small couplings $\sqrt{g_\nu g_e} \sim 3 \times 10^{-7}$ are preferred to explain the XENON1T excess. In such a small coupling region, the ν - e scattering mediated by the off-shell Z' is negligible compared to the weak interactions at around the neutrino decoupling temperature, $T_{\nu\text{-dec}} = \mathcal{O}(1)$ MeV. Thus, we ignore the Z' mediated scattering process.

We set the following initial conditions of the Boltzmann equations at $T_{\text{init}} = T_{\gamma e} = T_\nu = 20$ MeV,

$$f_{Z'} = 0 , \quad (24)$$

$$\rho_{\gamma e} = \rho_\gamma^{\text{BE}}(T_{\text{init}}) + \rho_e^{\text{FD}}(T_{\text{init}}) + \rho_{\gamma e}^{\text{QED}}(T_{\text{init}}) , \quad (25)$$

$$\rho_\nu = \rho_\nu^{\text{FD}}(T_{\text{init}}, 0) , \quad (26)$$

$$n_\nu = n_\nu^{\text{FD}}(T_{\text{init}}, 0) , \quad (27)$$

where $\rho_{\gamma e}^{\text{QED}}$ is the QED loop correction to the electromagnetic energy density. We solve the Boltzmann equations, (11), (21), (22) and (23) numerically with binned $f_{Z'}$. We validated our numerical code by comparing with the thermalized limit discussed in the next section.

4 N_{eff} constraint

Here, we show the results for the freeze-in scenario of Z' . Fig. 3 shows the contour plots of N_{eff} on the (g_e, g_ν) plane for $m_{Z'} = 1 \text{ eV}, 10 \text{ eV}, 100 \text{ eV}, 1 \text{ keV}, 10 \text{ keV},$ and 100 keV . Here, N_{eff} is defined by,

$$N_{\text{eff}} = \frac{8}{7} \left(\frac{11}{4} \right)^{4/3} \frac{\rho_\nu + \rho_{Z'}}{\rho_\gamma}, \quad (28)$$

at $T_\gamma = 0.26 \text{ eV}$. In the figure, we show the contours of $N_{\text{eff}} \leq 10$. In each plot, the dark-orange (light-orange) shaded region shows the consistent region with the Planck CMB only (joint Planck+BAO) constraint, $N_{\text{eff}} = 2.92^{+0.36}_{-0.37}$ ($2.99^{+0.34}_{-0.33}$) at 95% C.L. [19]. The each blue band is the parameter region favored for the light vector mediator interpretation of the XENON1T excess [3], i.e., $\sqrt{g_e g_\nu} \sim 3 \times 10^{-7}$.³ The figure shows that N_{eff} in the favored region exceeds $N_{\text{eff}} = 5$ for $m_{Z'} \geq 1 \text{ eV}$.

It should be noted that the massive mediator becomes long-lived enough to behave like “dark matter” at the recombination time in the region below the purple dashed lines. In this case, the above N_{eff} constraint cannot be applied. However, since such a region is far off from the favored region for the XENON1T excess, our conclusions are not affected.

In addition to the N_{eff} constraint, there is also a constraint on Z' with a mass $m_{Z'} \lesssim 100 \text{ eV}$ from neutrino free-streaming, due to the on-shell production of $\nu\nu \rightarrow Z'$. The mean free path of ν is affected by the partial decay rate of Z' into the neutrinos [31, 32]. We show the 95% C.L. bound of this effect in the Fig. 3 with the green shaded line. We mapped the constraint of Ref. [32] by matching the Majoron ϕ partial decay rate and Z' decay rate (8).⁴

As we discussed in Sec. 2, the mediator production through $e^\pm + \gamma \leftrightarrow e^\pm + Z'$ and $e^+ + e^- \leftrightarrow \gamma + Z'$ become less effective for $g_e \ll 10^{-10}$. The mediator production through $\nu + \nu \leftrightarrow Z' + Z'$ also becomes less effective for $g_\nu \ll 10^{-5}$. On the other hand, the mediator production via the inverse decay remains effective as long as g_ν satisfies the inequality in Eq. (9). Let us summarize the expected value of N_{eff} when Z' is thermalized for various parameter regions.

³In Ref. [3], the mediator universally couples to the three flavors of the neutrinos. Since our constraints are on the mediator coupling to one flavor neutrino, we scale the $(g_\nu g_e)^{1/2}$ in the favored region by a factor $\sim \sqrt{2}$.

⁴In this conversion, we take the difference of the degrees of freedom of Z' and the Majoron ϕ into account, by multiplying a factor 3, and average over neutrino flavors due to the neutrino oscillation, by dividing by another factor 3.

$$\frac{\lambda^2}{16\pi} m_\phi = \Gamma_{Z' \rightarrow \nu_e \nu_e}^0, \quad (29)$$

where m_ϕ is a Majoron mass and λ is a Majoron-neutrino coupling constant.

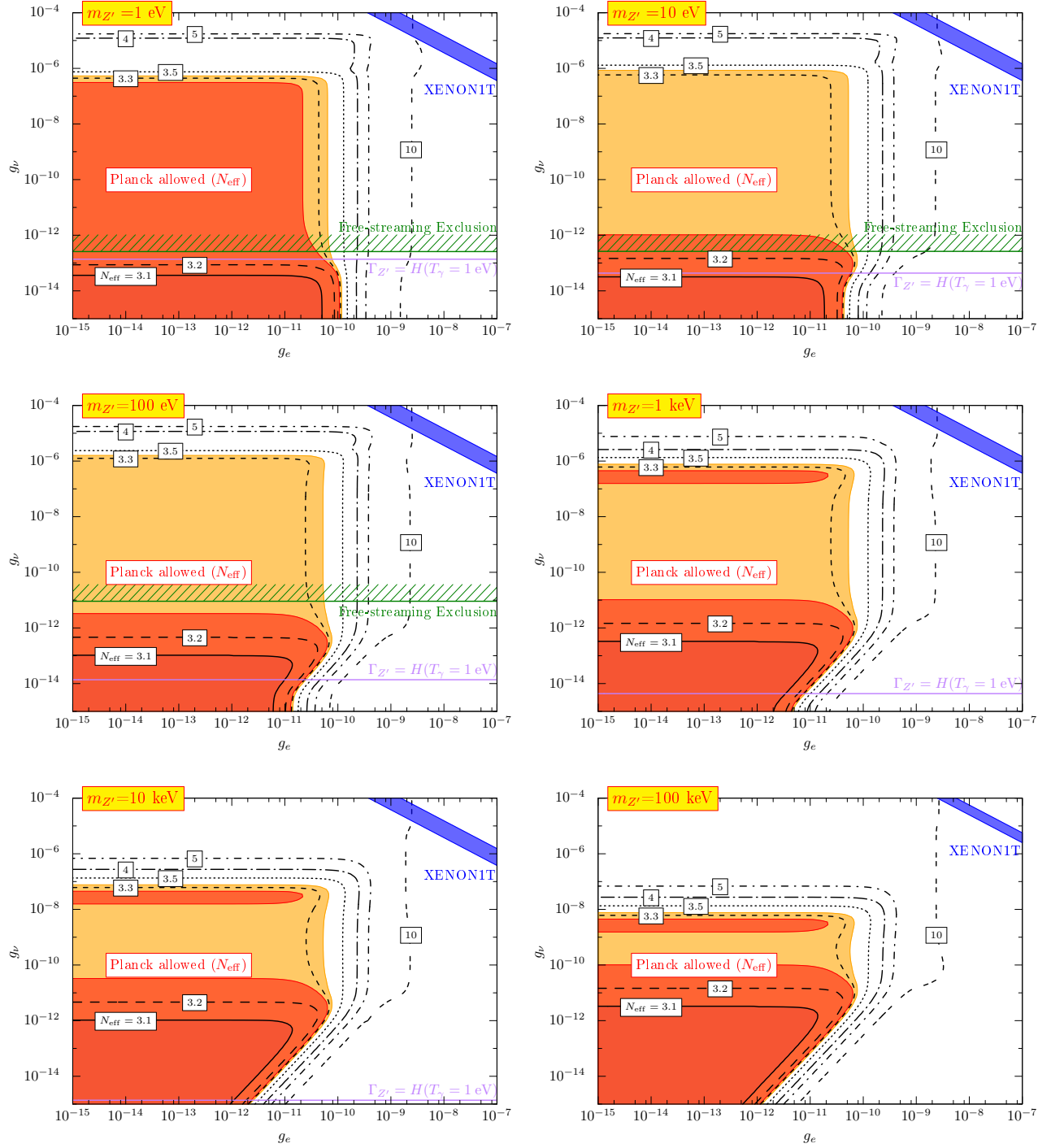
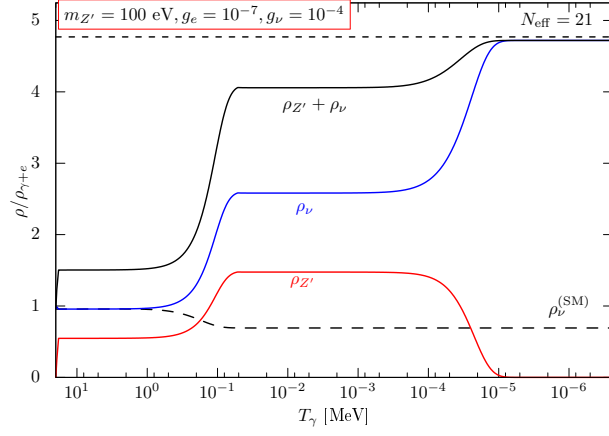
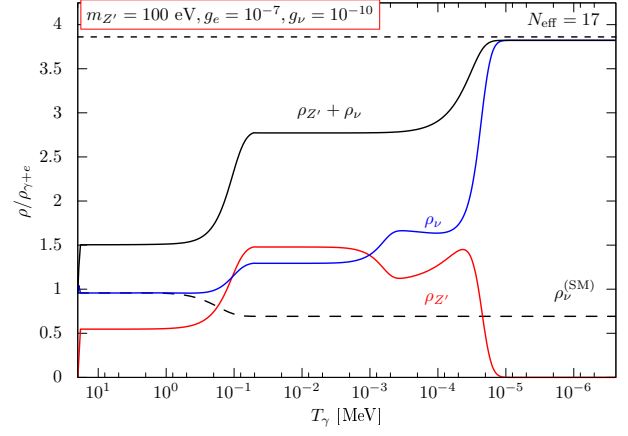


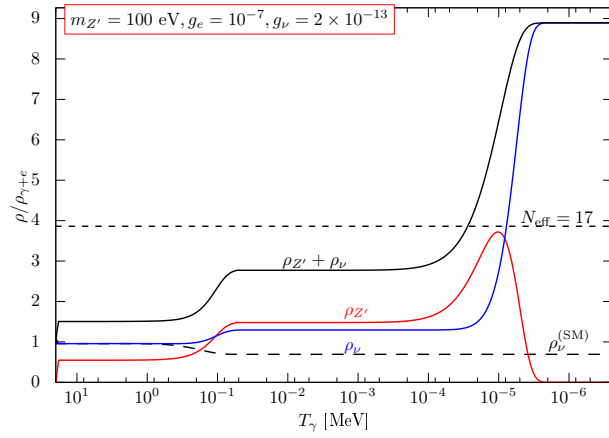
Figure 3: The contour plot of N_{eff} on the (g_e, g_ν) plane for a given mediator mass. Here, we assume that the mediator couples to one flavor of the three neutrinos. The dark-orange (light-orange) shaded regions are consistent with the Planck CMB only (joint Planck+BAO) constraint, $N_{\text{eff}} = 2.92^{+0.36}_{-0.37}$ ($2.99^{+0.34}_{-0.33}$) at 95% C.L. The green line corresponds to the neutrino free-streaming bound [32]. The blue bands are the regions favored by the XENON1T excess. The horizontal purple lines show the parameter at which the total decay rate of the Z' boson is compatible with the Hubble rate at the CMB era in the standard cosmology.



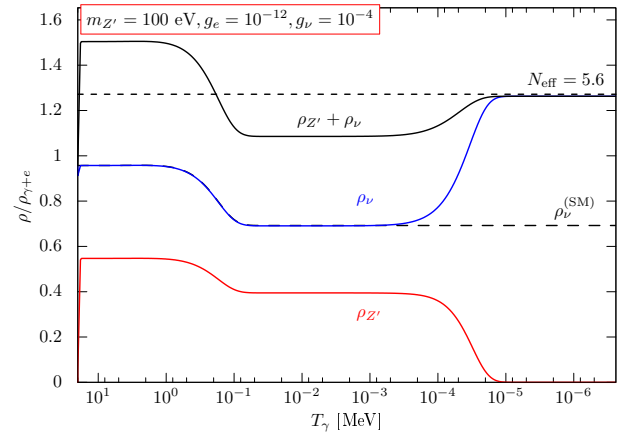
(a) Case (i)



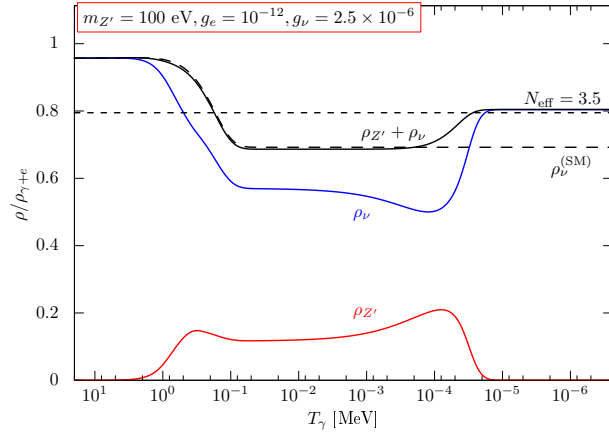
(b) Case (ii)



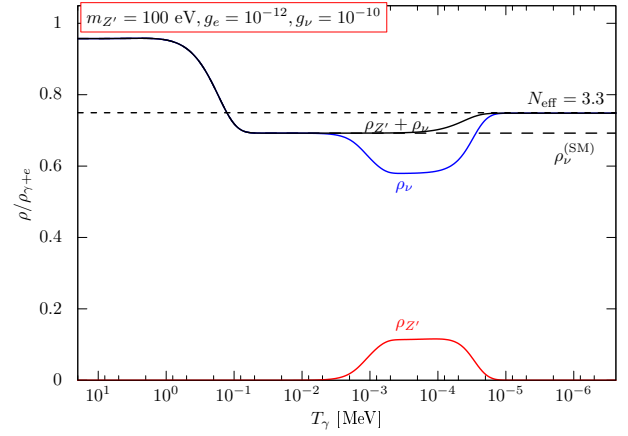
(c) Case (iii)



(d) Case (iv)



(e) Case (v)-1



(f) Case (v)-2

Figure 4: Time evolution of the energy densities which show the similar behaviors of the Cases (i-v).

(i) Simultaneous thermalization with both e^\pm and ν

For $g_e \gg 10^{-8}$ and $g_\nu \gg 10^{-5}$, the on-shell productions of the mediator from the γ - e thermal bath and the neutrino thermal bath are both effective, which delay the neutrino decoupling from the γ - e thermal bath until $T \lesssim m_e$. As a result, $T_\nu \simeq T_\gamma$ is kept until Z' annihilates away. Then, the in-equilibrium decay of the mediator before the recombination heats up the neutrino temperature relative to the photon temperature by a factor of

$$T_\nu = \left(\frac{\frac{7}{8} \times 2N_F + d_{Z'}}{\frac{7}{8} \times 2N_F} \right)^{1/3} T_\gamma = \left(\frac{11}{7} \right)^{1/3} T_\gamma , \quad (30)$$

where $N_F = 3$ is the number of flavors of the neutrinos and $d_{Z'} = 3$ is a spin degrees of freedom of Z' . Here, we have used the conservation of the entropy per comoving volume in the ν - Z' thermal bath. As a result, the expected N_{eff} for $g_e \gg 10^{-8}$ and $g_\nu \gg 10^{-5}$ is given by,

$$N_{\text{eff}} \simeq 3 \times \left(\frac{11}{4} \right)^{4/3} \times \left(\frac{11}{7} \right)^{4/3} \simeq 21 . \quad (31)$$

The first factor is due to the delay of the neutrino decoupling, i.e. $T_\nu \simeq T_\gamma$, while the second factor is due to the in-equilibrium decay of Z' . In Fig. 4a, we show the time evolution of the energy densities of ν and Z' for $g_e = 10^{-7}$, $g_\nu = 10^{-4}$ and $m_{Z'} = 100$ eV.

For $m_{Z'} \ll 1$ eV, Z' behaves as the dark radiation without heating up the ν temperature. In such a case, the expected N_{eff} is given by,

$$N_{\text{eff}} \simeq \left(\frac{11}{4} \right)^{4/3} \left(N_F + \frac{1}{2} \times \frac{8}{7} \times d_{Z'} \right) \simeq 18 , \quad (32)$$

where the second term in the last parenthesis denotes the Z' energy density.

(ii) Thermalization with e^\pm followed by ν -inverse decay

For $g_e \gg 10^{-8}$ but for $g_\nu \ll 10^{-5}$ while satisfying the condition in Eq. (9), the mediator remains in equilibrium with γ - e , even after the neutrino decouples as in the standard cosmology. In this case, the temperature of the γ - Z' thermal bath after the electron annihilation is given by,

$$T_\gamma = T_{Z'} = \left(\frac{\frac{7}{8} \times 4 + 2 + d_{Z'}}{2 + d_{Z'}} \right)^{1/3} T_\nu = \left(\frac{17}{10} \right)^{1/3} T_\nu . \quad (33)$$

After e^\pm have annihilated away, the (inverse) decay of Z' into the neutrinos becomes effective. The (inverse) decay changes the temperature and the chemical potential of ν - Z' thermal bath as

$$\rho_\nu(T_\nu, 0) + \rho_{Z'}((17/10)^{1/3} T_\nu, 0) = \rho_\nu(T_{\nu-Z'}, \mu_{\nu-Z'}) + \rho_{Z'}(T_{\nu-Z'}, 2\mu_{\nu-Z'}) , \quad (34)$$

$$n_\nu(T_\nu, 0) + 2n_{Z'}((17/10)^{1/3} T_\nu, 0) = n_\nu(T_{\nu-Z'}, \mu_{\nu-Z'}) + 2n_{Z'}(T_{\nu-Z'}, 2\mu_{\nu-Z'}) , \quad (35)$$

for $\mu_{\nu-Z'} < 0$. For $\mu_{\nu-Z'} \rightarrow 0$, on the other hand, the conditions are given by

$$\rho_\nu(T_\nu, 0) + \rho_{Z'}((17/10)^{1/3}T_\nu, 0) = \rho_\nu(T_{\nu-Z'}, 0) + \rho_{Z'}(T_{\nu-Z'}, 0) , \quad (36)$$

$$n_\nu(T_\nu, 0) + 2n_{Z'}((17/10)^{1/3}T_\nu, 0) = n_\nu(T_{\nu-Z'}, 0) + 2n_{Z'}(T_{\nu-Z'}, 0) + 2n_{Z'}^{(0)} . \quad (37)$$

Here, T_ν denotes the neutrino temperature in the absence of the inverse decay of Z' . The mediator distribution is approximated by the Bose-Einstein distribution of the massless particle with the temperature T and the chemical potential μ . The first and the second arguments of the energy/number densities are the temperature and the chemical potential, respectively. The zero momentum contribution to the number density is denoted by $n_{Z'}^{(0)}$, of which the energy density is neglected in the massless approximation. The conditions in Eqs. (35) and (37) are due to the conservation of $n_\nu + 2n_{Z'}$ in the (inverse) decay process, which also imposes $\mu_{Z'} = 2\mu_\nu$. The above conditions lead to

$$T_{\nu-Z'} \simeq 1.1 T_\nu , \quad \mu_{\nu-Z'} = 0 , \quad n_{Z'}^{(0)} \simeq 0.084 T_\nu^3 . \quad (38)$$

The result in Eq. (38) shows that Z' exhibits a dilute Bose-Einstein condensation (BEC). In the presence of the BEC, the zero momentum contribution should be treated properly in the Boltzmann equation (see, e.g., Refs. [33, 34]). In our numerical analysis, however, we use the Boltzmann equation neglecting the zero momentum contribution. Since $n_{Z'}^{(0)}$ is subdominant, our approximation fairly reproduces the expected N_{eff} discussed below (see also Fig. 4b).

The in-equilibrium decay of Z' before the CMB era heats up the neutrino temperature as

$$s_\nu(T_{\nu-Z'}, 0) + s_{Z'}(T_{\nu-Z'}, 0) = s_\nu(T'_\nu, \mu'_\nu) , \quad (39)$$

$$n_\nu(T_{\nu-Z'}, 0) + 2n_{Z'}(T_{\nu-Z'}, 0) + 2n_{Z'}^{(0)} = n_\nu(T'_\nu, \mu'_\nu) . \quad (40)$$

The resultant temperature and the chemical potential of ν are given by,

$$T'_\nu \simeq 0.76 T_\nu , \quad \mu'_\nu \simeq 1.9 T_\nu , \quad (41)$$

where T_ν is again the neutrino temperature in the absence of the inverse decay nor the decay of Z' . As a result, we find⁵

$$N_{\text{eff}} \simeq 17 . \quad (42)$$

In Fig. 4b, we show the time evolution of the energy densities of ν and Z' for $g_e = 10^{-7}$, $g_\nu = 10^{-10}$ and $m_{Z'} = 100$ eV.

For $m_{Z'} \ll 1$ eV, the decay of Z' takes place after the recombination, and hence, it contributes to N_{eff} as dark radiation as in the previous case. The resultant N_{eff} is given by,

$$N_{\text{eff}} \simeq 12 . \quad (43)$$

⁵For $d_{Z'} = 1$, for example, we find $N_{\text{eff}} = 12$ for $m_{Z'} \geq 1$ eV and $N_{\text{eff}} = 11$ for $m_{Z'} \ll 1$ eV.

(iii) Thermalization with e^\pm followed by out-of-equilibrium decay of Z'

For $g_e \gg 10^{-9}$ and $\Gamma_{Z'} \ll H(T \simeq m_{Z'})$, Z' exhibits the non-equilibrium decay. In this case, the ν energy density is more enhanced than that expected from Eqs. (39) and (40), and hence,

$$N_{\text{eff}} > 17 . \quad (44)$$

In Fig. 4c, we show the time evolution of the energy densities of ν and Z' for $g_e = 10^{-7}$, $g_\nu = 2 \times 10^{-13}$ and $m_{Z'} = 100$ eV.

For $m_{Z'} \ll 1$ eV, N_{eff} is again given by,

$$N_{\text{eff}} \simeq 12 , \quad (45)$$

since Z' is effectively an massless degree of freedom at the recombination.

(iv) Thermalization with ν before neutrino decoupling

For $g_\nu \gg 10^{-5}$ and $g_e \ll 10^{-9}$, the production of Z' from e^\pm is not significant, while it is in equilibrium with the neutrino thermal bath. When Z' is thermalized with ν before the neutrino decoupling, the temperature of ν - Z' thermal bath is given by

$$T_{\nu-Z'} \simeq \left(\frac{4}{11} \right)^{1/3} T_\gamma , \quad (46)$$

with the vanishing chemical potential after e^\pm annihilates away.

After the in-equilibrium decay of Z' , the neutrino temperature is enhanced by a factor in Eq. (30),

$$T_\nu = \left(\frac{\frac{7}{8} \times 2N_F + d_{Z'}}{\frac{7}{8} \times 2N_F} \right)^{1/3} T_{\nu-Z'} = \left(\frac{11}{7} \right)^{1/3} T_{\nu-Z'} , \quad (47)$$

where $T_{\nu-Z'}$ is the temperature without the in-equilibrium decay of Z' . As a result, we obtain

$$N_{\text{eff}} \simeq N_{\text{eff}}^{(\text{SM})} \times \left(\frac{\frac{7}{8} \times 2N_F + d_{Z'}}{\frac{7}{8} \times 2N_F} \right)^{4/3} \simeq 5.6 . \quad (48)$$

In Fig. 4d, we show the time evolution of the energy densities of ν and Z' for $g_e = 10^{-12}$, $g_\nu = 10^{-4}$ and $m_{Z'} = 100$ eV.

For $m_{Z'} \ll 1$ eV, the mediator contributes to N_{eff} as a dark radiation with the temperature in Eq. (46). As a result, N_{eff} is given by,

$$N_{\text{eff}} \simeq N_{\text{eff}}^{(\text{SM})} \times \left(\frac{\frac{7}{8} \times 2N_F + d_{Z'}}{\frac{7}{8} \times 2N_F} \right) \simeq 4.8 . \quad (49)$$

(v) Thermalization with ν after neutrino decoupling

For $g_e \ll 10^{-9}$ and $g_\nu \lesssim 10^{-5}$, the thermalization with neutrino takes place after the neutrino decoupling. Although such parameter region is far off from that favored by the XENON1T excess (see Fig. 3), let us briefly comment on the behavior of N_{eff} in this region.

For g_ν with which both the $\nu + \nu \leftrightarrow Z'$ and $\nu + \nu \leftrightarrow Z' + Z'$ are effective (see Eqs. (6) and (9)), the chemical potentials of ν and Z' vanish. Hence, the energy density of ν and Z' after thermalization is determined by,

$$\rho_\nu(T_\nu, 0) = \rho_\nu(T_{\nu-Z'}, 0) + \rho_{Z'}(T_{\nu-Z'}, 0) . \quad (50)$$

Thus, the temperature of the ν - Z' thermal bath is given by,

$$T_{\nu-Z'} = \left(\frac{\frac{7}{8} \times 2N_F}{\frac{7}{8} \times 2N_F + d_{Z'}} \right)^{1/4} T_\nu = \left(\frac{7}{11} \right)^{1/4} T_\nu . \quad (51)$$

After the in-equilibrium decay of Z' , the neutrino temperature is heat up by a factor of $(11/7)^{1/3}$. As a result, we find

$$N_{\text{eff}} \simeq N_{\text{eff}}^{(\text{SM})} \times \left(\frac{7}{11} \right) \times \left(\frac{11}{7} \right)^{4/3} \simeq 3.5 . \quad (52)$$

In Fig. 4e, we show the time evolution of the energy densities of ν and Z' for $g_e = 10^{-12}$, $g_\nu = 2.5 \times 10^{-6}$ and $m_{Z'} = 100$ eV.

For $g_\nu \ll 10^{-5}$ but satisfying the condition in Eq. (9), $\nu + \nu \leftrightarrow Z' + Z'$ is irrelevant, while $\nu + \nu \leftrightarrow Z'$ is effective. In this case, the temperature and the chemical potential of the ν - Z' thermal bath are determined by

$$\rho_\nu(T_\nu, 0) = \rho_\nu(T_{\nu-Z'}, \mu_{\nu-Z'}) + \rho_{Z'}(T_{\nu-Z'}, 2\mu_{\nu-Z'}) , \quad (53)$$

$$n_\nu(T_\nu, 0) = n_\nu(T_{\nu-Z'}, \mu_{\nu-Z'}) + 2n_{Z'}(T_{\nu-Z'}, 2\mu_{\nu-Z'}) . \quad (54)$$

The resultant temperature and the chemical potential of ν are given by,

$$T_{\nu-Z'} \simeq 1.2 T_\nu , \quad \mu_{\nu-Z'} \simeq -1.2 T_\nu . \quad (55)$$

Here, T_ν is again the neutrino temperature in the absence of the (inverse) decay of Z' .

Then, the in-equilibrium decay of Z' before the recombination heats up the neutrino temperature as,

$$s_\nu(T_{\nu-Z'}, \mu_{\nu-Z'}) + s_{Z'}(T_{\nu-Z'}, 2\mu_{\nu-Z'}) = s_\nu(T'_\nu, \mu'_\nu) , \quad (56)$$

$$n_\nu(T_{\nu-Z'}, \mu_{\nu-Z'}) + 2n_{Z'}(T_{\nu-Z'}, 2\mu_{\nu-Z'}) = n_\nu(T'_\nu, \mu'_\nu) . \quad (57)$$

The resultant temperature and the chemical potential of ν are given by,

$$T'_\nu \simeq 1.1 T_\nu , \quad \mu'_\nu \simeq -0.31 T_\nu . \quad (58)$$

As a result, we find

$$N_{\text{eff}} \simeq 3.3, \quad (59)$$

which is consistent with the joint Planck+BAO constraint on N_{eff} at 95% C.L., while it is excluded by the CMB only constraint at 95% C.L. In Fig. 4f, we show the time evolution of the energy densities of ν and Z' for $g_e = 10^{-12}$, $g_\nu = 10^{-10}$ and $m_{Z'} = 100$ eV.

For $m_{Z'} \ll 1$ eV, the mediator Z' contributes to N_{eff} as a dark radiation. However, due to the energy conservation in Eq. (53), the total energy density of the $\nu + Z'$ is the same with that of ν in the standard cosmology, and hence,

$$N_{\text{eff}} = N_{\text{eff}}^{(\text{SM})}. \quad (60)$$

Thus, for $m_{Z'} \ll 1$ eV, $g_\nu \ll 10^{-5}$ and $g_e \ll 10^{-9}$, the mediator is not constrained by the N_{eff} observation, even if the mediator is thermalized by the inverse decay of the neutrinos. We summarize the each case of the above and the corresponding asymptotic values of N_{eff} in Fig. 5.

It should be noted that the cases (i)–(iv) are also constrained by the Big-Bang Nucleosynthesis (BBN) since the energy density $\rho_\nu + \rho_{Z'}$ deviates from ρ_ν in the standard cosmology at $T_\gamma < \mathcal{O}(0.1)$ MeV. Typically, the BBN constraint on $|\Delta N_{\text{eff}}|$ is about 0.3 at 68% C.L. [35, 36], which is slightly weaker than the CMB constraint. In the case (v), on the other hand, the energy density $\rho_\nu + \rho_{Z'}$ is the same with ρ_ν in the standard cosmology for $T_\nu \gg m_{Z'}$ (see e.g. Ref. [37]). Thus, the BBN constraints can be evaded for a very light Z' . As we have seen, for such a very light Z' with $m_{Z'} \lesssim 100$ eV, there is a constraint from the neutrino free-streaming on the CMB in which the interaction between Z' and the neutrinos reduces the free-streaming length [31, 32].

5 Conclusions

In this paper, we discussed the constraints on the light vector mediator interpretation of the XENON1T excess from N_{eff} . This interpretation favors the mediator with a mass $m_{Z'} < \mathcal{O}(100)$ keV and the electron/neutrino coupling $(g_e g_\nu)^{1/2} \simeq 3 \times 10^{-7}$ [3]. By solving the Boltzmann equation of the momentum distribution of the mediator, we find that the favored parameter region results in $N_{\text{eff}} > 5$ for $m_{Z'} \geq 1$ eV, which exceeds the current upper limit on N_{eff} . By combined with the very conservative constraint from the stellar cooling on the light mediator coupling to the electron in Ref. [12, 16], we conclude that the light vector mediator interpretation is not valid anymore.

In this paper, we considered the case of the vector mediators. To explain the XENON1T excess, the scalar mediator models have been also proposed. For those model, we can apply N_{eff} constraint in a similar manner. However, the thermal history of those cases depends on the detail of the models such as the presence of the right-handed neutrinos. Although detailed analyses are out of scope of this work, our results of the thermalized cases (i)–(iv) can be applied straightforwardly by replacing $d_{Z'} = 3$ to $d_{Z'} = 1$. In these cases, the mediator couplings favored by the XENON1T excess seem

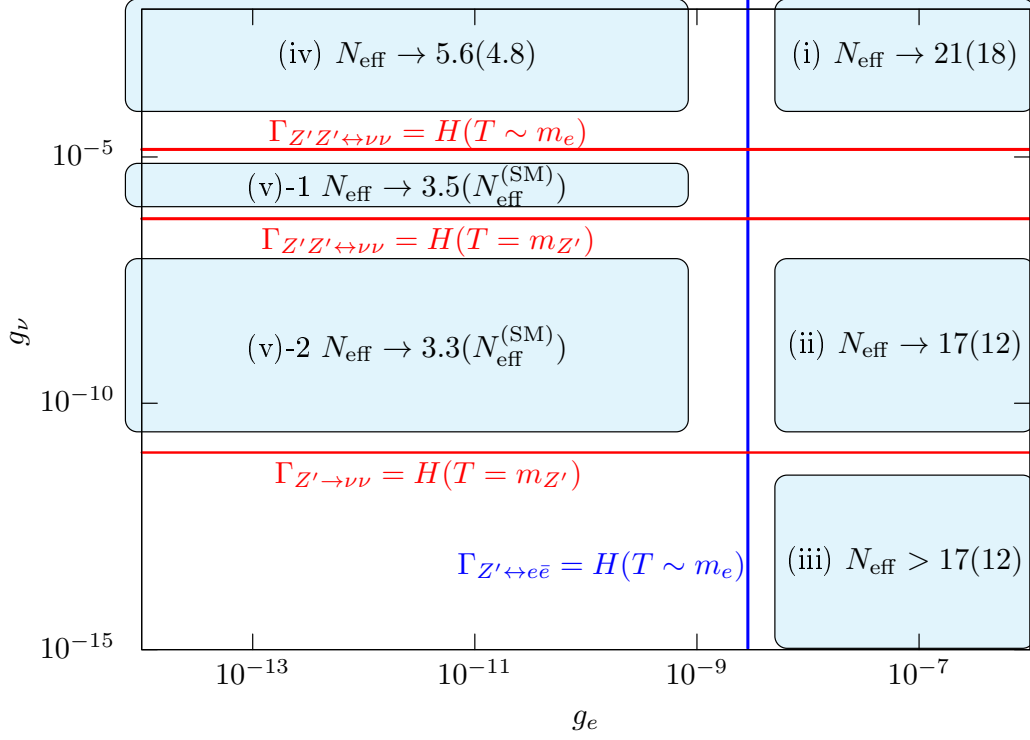


Figure 5: Schematic picture of summary of the each case study of the section 4.

to be in strong tension with the N_{eff} constraint. For the detail analysis, we will discuss these cases elsewhere.

Acknowledgments

This work is supported by Grant-in-Aid for Scientific Research from the Ministry of Education, Culture, Sports, Science, and Technology (MEXT), Japan, 17H02878 (M.I. and S.S.), 18H05542 (M.I.), 18K13535, 19H04609 and 20H01895 (S.S.), and by World Premier International Research Center Initiative (WPI), MEXT, Japan. This work is also supported by the Advanced Leading Graduate Course for Photon Science (S.K.), the JSPS Research Fellowships for Young Scientists (S.K.) and International Graduate Program for Excellence in Earth-Space Science (Y.N.).

A Neutrino-Electron Collision Terms

Here, we present the explicit form of the collision terms for neutrino-electron scatterings used in this work. In the text, we define the collision terms of these processes for the zeroth and first moment

$$C_{e\leftrightarrow\nu}^{(j)} = \sum_{i=e,\mu,\tau} C_{e\leftrightarrow\nu_i}^{(j)}, \quad j = 0, 1 \quad (61)$$

$$C_{e\leftrightarrow\nu_i}^{(0)} = \int \frac{g_{\nu_i} d^3 p_{\nu_i}}{(2\pi)^3} (\mathcal{C}_{e^+e^-\leftrightarrow\nu_i\bar{\nu}_i} + \mathcal{C}_{e^\pm\nu_i\leftrightarrow e^\pm\nu_i} + \mathcal{C}_{e^\pm\bar{\nu}_i\leftrightarrow e^\pm\bar{\nu}_i}) , \quad (62)$$

$$C_{e\leftrightarrow\nu_i}^{(1)} = \int \frac{g_{\nu_i} d^3 p_{\nu_i}}{(2\pi)^3} p_{\nu_i} (\mathcal{C}_{e^+e^-\leftrightarrow\nu_i\bar{\nu}_i} + \mathcal{C}_{e^\pm\nu_i\leftrightarrow e^\pm\nu_i} + \mathcal{C}_{e^\pm\bar{\nu}_i\leftrightarrow e^\pm\bar{\nu}_i}) . \quad (63)$$

Using the results of Appendix A.3 of Ref. [25], these are written in the form of

$$C_{e\leftrightarrow\nu}^{(0)} = 8f_n^{\text{FD}} \frac{G_F^2}{\pi^5} (3 - 4s_W^2 + 24s_W^4) (T_\gamma^8 - T_\nu^8 e^{\frac{2\mu_\nu}{T_\nu}}) , \quad (64)$$

$$C_{e\leftrightarrow\nu}^{(1)} = \frac{G_F^2}{\pi^5} (3 - 4s_W^2 + 24s_W^4) G(T_\gamma, 0, T_\nu, \mu_\nu) , \quad (65)$$

where G_F is the Fermi constant, s_W is the sine of the Weinberg angle, and $f_n^{\text{FD}} = 0.852$. The function $G(T_1, \mu_1, T_2, \mu_2)$ is given by

$$G(T_1, \mu_1, T_2, \mu_2) = 32f_a^{\text{FD}} (T_1^9 e^{\frac{2\mu_1}{T_1}} - T_2^9 e^{\frac{2\mu_2}{T_2}}) + 56f_s^{\text{FD}} e^{\frac{\mu_1}{T_1}} e^{\frac{\mu_2}{T_2}} T_1^4 T_2^4 (T_1 - T_2) , \quad (66)$$

where the numerical factors $f_a^{\text{FD}} = 0.884$ and $f_s^{\text{FD}} = 0.829$ represent the Pauli blocking effect from the Fermi-Dirac distribution in the annihilation and scattering processes, respectively. Note that we assume that each neutrino flavor has the same temperature and chemical potential.

References

- [1] E. Aprile *et al.* (XENON), (2020), arXiv:2006.09721 [hep-ex] .
- [2] L. Di Luzio, M. Fedele, M. Giannotti, F. Mescia, and E. Nardi, (2020), arXiv:2006.12487 [hep-ph] .
- [3] C. Boehm, D. G. Cerdeno, M. Fairbairn, P. A. Machado, and A. C. Vincent, (2020), arXiv:2006.11250 [hep-ph] .
- [4] d. Amaral, Dorian Warren Praia, D. G. Cerdeno, P. Foldenauer, and E. Reid, (2020), arXiv:2006.11225 [hep-ph] .
- [5] A. Bally, S. Jana, and A. Trautner, (2020), arXiv:2006.11919 [hep-ph] .
- [6] D. Aristizabal Sierra, V. De Romeri, L. Flores, and D. Papoulias, (2020), arXiv:2006.12457 [hep-ph] .

- [7] A. N. Khan, (2020), arXiv:2006.12887 [hep-ph] .
- [8] M. Lindner, Y. Mambrini, T. B. d. Melo, and F. S. Queiroz, (2020), arXiv:2006.14590 [hep-ph] .
- [9] S. A. Díaz, K.-P. Schröder, K. Zuber, D. Jack, and E. E. B. Barrios, “Constraint on the axion-electron coupling constant and the neutrino magnetic dipole moment by using the tip-rgb luminosity of fifty globular clusters,” (2019), arXiv:1910.10568 [astro-ph.SR] .
- [10] J. Grifols and E. Masso, Phys. Lett. B **173**, 237 (1986).
- [11] J. Grifols, E. Masso, and S. Peris, Mod. Phys. Lett. A **4**, 311 (1989).
- [12] H. An, M. Pospelov, and J. Pradler, Physics Letters B **725**, 190–195 (2013).
- [13] J. Redondo and G. Raffelt, Journal of Cosmology and Astroparticle Physics **2013**, 034–034 (2013).
- [14] J. H. Chang, R. Essig, and S. D. McDermott, JHEP **01**, 107 (2017), arXiv:1611.03864 [hep-ph] .
- [15] J. H. Chang, R. Essig, and S. D. McDermott, JHEP **09**, 051 (2018), arXiv:1803.00993 [hep-ph] .
- [16] J. Redondo, JCAP **07**, 008 (2008), arXiv:0801.1527 [hep-ph] .
- [17] P. F. de Salas and S. Pastor, JCAP **1607**, 051 (2016), arXiv:1606.06986 [hep-ph] .
- [18] K. Akita and M. Yamaguchi, (2020), arXiv:2005.07047 [hep-ph] .
- [19] N. Aghanim *et al.* (Planck), (2018), arXiv:1807.06209 [astro-ph.CO] .
- [20] R. Foot, Mod. Phys. Lett. A **6**, 527 (1991).
- [21] X.-G. He, G. C. Joshi, H. Lew, and R. Volkas, Phys. Rev. D **44**, 2118 (1991).
- [22] B. Holdom, Phys. Lett. B **166**, 196 (1986).
- [23] M. Ibe, S. Kobayashi, Y. Nakayama, and S. Shirai, JHEP **04**, 009 (2020), arXiv:1912.12152 [hep-ph] .
- [24] M. Escudero, D. Hooper, G. Krnjaic, and M. Pierre, JHEP **03**, 071 (2019), arXiv:1901.02010 [hep-ph] .
- [25] M. Escudero Abenza, JCAP **05**, 048 (2020), arXiv:2001.04466 [hep-ph] .
- [26] M. Escudero, JCAP **02**, 007 (2019), arXiv:1812.05605 [hep-ph] .

- [27] S. D. McDermott, H. H. Patel, and H. Ramani, Physical Review D **97** (2018), 10.1103/phys-revd.97.073005.
- [28] A. F. Heckler, Phys. Rev. **D49**, 611 (1994).
- [29] N. Fornengo, C. W. Kim, and J. Song, Phys. Rev. **D56**, 5123 (1997), arXiv:hep-ph/9702324 [hep-ph] .
- [30] G. Mangano, G. Miele, S. Pastor, and M. Peloso, Phys. Lett. **B534**, 8 (2002), arXiv:astro-ph/0111408 [astro-ph] .
- [31] Z. Chacko, L. J. Hall, T. Okui, and S. J. Oliver, Phys. Rev. D **70**, 085008 (2004), arXiv:hep-ph/0312267 .
- [32] M. Escudero and S. J. Witte, Eur. Phys. J. C **80**, 294 (2020), arXiv:1909.04044 [astro-ph.CO] .
- [33] D. Semikoz and I. Tkachev, Phys. Rev. Lett. **74**, 3093 (1995), arXiv:hep-ph/9409202 .
- [34] D. Semikoz and I. Tkachev, Phys. Rev. D **55**, 489 (1997), arXiv:hep-ph/9507306 .
- [35] C. Pitrou, A. Coc, J.-P. Uzan, and E. Vangioni, Phys. Rept. **754**, 1 (2018), arXiv:1801.08023 [astro-ph.CO] .
- [36] B. D. Fields, K. A. Olive, T.-H. Yeh, and C. Young, JCAP **03**, 010 (2020), arXiv:1912.01132 [astro-ph.CO] .
- [37] A. Berlin, N. Blinov, and S. W. Li, Phys. Rev. D **100**, 015038 (2019), arXiv:1904.04256 [hep-ph] .